Caveolin Plays a Central Role in Endothelial Progenitor Cell Mobilization and Homing in SDF-1–Driven Postischemic Vasculogenesis

Elhem Sbaa, Julie DeWever, Philippe Martinive, Caroline Bouzin, Françoise Frérart, Jean-Luc Balligand, Chantal Dessy and Olivier Feron

Circ. Res. 2006;98;1219-1227; originally published online Apr 6, 2006;
DOI: 10.1161/01.RES.0000220648.80170.8b
Circulation Research is published by the American Heart Association. 7272 Greenville Avenue, Dallas, TX 72514
 Print ISSN: 0009-7330. Online ISSN: 1524-4571

Caveolin Plays a Central Role in Endothelial Progenitor Cell Mobilization and Homing in SDF-1–Driven Postischemic Vasculogenesis

Elhem Sbaa, Julie DeWever, Philippe Martinive, Caroline Bouzin, Françoise Frérart, Jean-Luc Balligand, Chantal Dessy, Olivier Feron

***Abstract*—**When neovascularization is triggered in ischemic tissues, angiogenesis but also (postnatal) vasculogenesis is induced, the latter requiring the mobilization of endothelial progenitor cells (EPC) from the bone marrow. Caveolin, the structural protein of caveolae, was recently reported to directly influence the angiogenic process through the regulation of the vascular endothelial growth factor (VEGF)/nitric oxide pathway. In this study, using caveolin-1 null mice ($Cav^{-/-}$), we examined whether caveolin was also involved in the EPC recruitment in a model of ischemic hindlimb. Intravenous infusion of Sca-1^{+} Lin^{-} progenitor cells, but not bone marrow transplantation, rescued the defective neovascularization in $Cav^{-/-}$ mice, suggesting a defect in progenitor mobilization. The adhesion of $Cav^{-/-}$ EPC to bone marrow stromal cells indeed appeared to be resistant to the otherwise mobilizing SDF-1 (Stromal cell–Derived Factor-1) exposure because of a defect in the internalization of the SDF-1 cognate receptor CXCR4. Symmetrically, the attachment of $Cav^{-/-}$ EPC to SDF-1–presenting endothelial cells was significantly increased. Finally, EPC transduction with caveolin small interfering RNA reproduced this advantage in vitro and, importantly, led to a more extensive rescue of the ischemic hindlimb after intravenous infusion (versus sham-transfected EPC). These results underline the critical role of caveolin in ensuring the caveolae-mediated endocytosis of CXCR4, regulating both the SDF-1–mediated mobilization and peripheral homing of progenitor cells in response to ischemia. In particular, a transient reduction in caveolin expression was shown to therapeutically increase the engraftment of progenitor cells. **(*Circ Res*. 2006;98:1219-1227.)**

Key Words: caveolin ■ caveolae ■ postnatal vasculogenesis ■ endothelial progenitor cells ■ ischemia

Vasculogenesis and angiogenesis are the 2 major processes contributing to neovascularization in adults.[1,2] Postnatal vasculogenesis in adults requires the recruitment of progenitor cells derived from the bone marrow,[3] whereas angiogenesis involves the proliferation and migration of endothelial cells from the preexisting vessels.[4] The proportion of either process in promoting the development of neovessels in pathological situations, such as ischemia and tumor growth, may vary and both are considered to be complementary.[3,5] Moreover, the 2 processes share biological mediators including chemocytokines and proteinases.[6]

Among the key players in postnatal vasculogenesis, SDF-1 (Stromal cell–Derived Factor-1) and vascular endothelial growth factor (VEGF) have undoubtedly been the focus of the most attention. Through specific interactions with the CXCR4 and VEGFR-2 receptors, SDF-1 and VEGF, respectively, contribute to increase the recruitment of progenitor cells from the bone marrow to the peripheral blood, thereby leading to the formation of new vessels at the ischemic sites.[2] Recently, we identified a critical role of caveolin-1 (a structural protein of caveolae) in the regulation of the VEGF-signaling pathway in a model of adaptive angiogenesis.[7] We found that the compartmentation of the VEGFR-2 receptor in caveolae was key to ensure VEGF-mediated neovascularization. Accordingly, genetic deletion of caveolin-1 (and the ensuing absence of caveolae) was found to alter the endothelial nitric oxide synthase (eNOS) and ERK-dependent pathways downstream of VEGF stimulation, thereby leading to a defect in angiogenesis. A key role of caveolin-1 in angiogenesis was also identified in mouse tumor models and in the implanted Matrigel plug assay,[8–10] mostly through the modulation of nitric oxide bioavailability. Notably, in none of these studies focusing on the role of caveolin in neovascularization was the potential impact of caveolin/caveolae in postnatal vasculogenesis (versus angiogenesis) addressed.

A series of indirect observations, however, argue for a role of caveolin in the bone marrow cell–dependent neovessel formation: (1) the activity of matrix metalloprotease-9 (MMP-9), a major protease involved in stem cell mobilization is modulated by nitric oxide,[11] the production of which is directly dependent on caveolin abundance[12]; (2) some proteins involved in the interaction between progenitor cells and bone marrow stroma, including adhesion molecules[13–15] and chemokine receptor,[16]

Original received September 28, 2005; resubmission received February 16, 2006; accepted March 27, 2006.
From the Unit of Pharmacology and Therapeutics, University of Louvain Medical School, Brussels, Belgium.
Correspondence to Olivier Feron, UCL-FATH5349, 53 Avenue E Mounier, B-1200 Brussels, Belgium. E-mail feron@mint.ucl.ac.be

Circulation Research **is available at http://circres.ahajournals.org** **DOI: 10.1161/01.RES.0000220648.80170.8b**

have already been associated to caveolae in other tissues; (3) the quasilinear relationship between caveolin expression and caveolae density,[17] and the capacity of caveolae to pinch off and to sequester their content[18] may account for the dynamic regulation of the expression of 1 or several of the abovementioned proteins at the cell surface.

Such evidence suggesting the potential role of caveolin/caveolae in progenitor cell biology and mobilization prompted us to explore the vasculogenic process in caveolin-deficient mice. More generally, another purpose of this study was to determine whether promotion of postnatal vasculogenesis could help rescue ischemic tissues in caveolin-null mice. Alteration in caveolin abundance has, indeed, been reported in many cardiovascular diseases that themselves are associated with a defect in angiogenesis.[19,20]

Materials and Methods

An expanded Materials and Methods section is provided in the online data supplement at http://circres.ahajournals.org.

Animals

Caveolin-deficient mice ($Cav^{-/-}$)[21] and their control littermates ($Cav^{+/+}$) were generated through heterozygous matings and housed in our local facility. Anesthetized mice underwent a double femoral artery and vein ligation to allow resection of 2-mm vessel segments under a stereoscopic microscope while innervation was carefully preserved.

Bone Marrow and Endothelial Progenitor Cells

Bone marrow mononuclear cells were isolated by separation onto a Ficoll Histopaque gradient (Sigma), and magnetic cell sorting (Miltenyi Biotech) was used for positive and/or negative selection to collect Sca-1^+/lineage marker-negative (Lin^-) cells or $CD45^+$ cells (BD Bioscience Pharmingen). For endothelial progenitor cell (EPC) production, bone marrow mononuclear cells were directly cultured on fibronectin-coated flasks using endothelial cell growth medium, as previously described.[22] The identity of EPC was confirmed by morphological and immunocytochemical analyses. EPC were used at day 7 after initial seeding except when indicated otherwise.

Results

Infusion of Sca-1^+ Lin^- Bone Marrow Cells Rescues Ischemic Hindlimb Perfusion in $Cav^{-/-}$ Mice

We have previously reported that after resection of 2 mm-femoral artery/vein segments, $Cav^{-/-}$ mice never restored a normal hindlimb perfusion, compared with wild-type mice that completely recovered[7] (see also below). To evaluate whether progenitor cells could help rescuing the impaired neovascularization in $Cav^{-/-}$ mice, we examined the effects of the infusion of Sca-1^+ Lin^- BMC on the restoration of the perfusion in the operated hindlimb. Serial examinations of blood flow by laser Doppler imaging were performed on days 3, 7, 10, and 14 (day 0 being fixed as the day of ligature). Figure 1A shows that infusion of 10^6 BMC issued either from wild-type ($Cav^{+/+}$) or $Cav^{-/-}$ mice did rescue the limb perfusion, whereas a permanent drop in blood flow was observed in the operated leg of untreated $Cav^{-/-}$ mice. Of note, in $Cav^{+/+}$ mice, infusion of $Cav^{+/+}$ BMC barely influenced the extent (and rate) of the otherwise naturally occurring reperfusion of the operated hindlimb (see Figure 1B).

In some experiments, we loaded BMC with a long-lasting tracker (carboxymethyl-1,1′-dioctadecyl-3,3,3′,3′-tetramethylindocarbocyanine [CM-DiI]) to follow their in vivo fate after infusion. Accordingly, histological analyses confirmed the presence of CM-DiI–labeled cells in the adductor muscle of $Cav^{-/-}$ mice, regardless of the $Cav^{-/-}$ or $Cav^{+/+}$ mouse origin of infused cells (Figure 1C). CM-DiI–labeled cells could be found as early as 24 hours after induction of ischemia and were still detectable at day 14 (at much lower level). It should, however, be noted that posttransplantation dilution of the tracker (with cell division) may lead to underestimation of progenitor cell recruitment at longer times. The CM-DiI overlapping with CD31-positive capillary endothelial cells amounted to 29±12% and 37±13% (of total CM-DiI staining) in experiments with $Cav^{-/-}$ and $Cav^{+/+}$ BMC, respectively (Figure 1C).

Ischemia-Induced Mobilization of $Cav^{-/-}$ Progenitor Cells Is Defective

Because infusion of $Cav^{-/-}$ BMC in $Cav^{-/-}$ mice did restore normal blood flow, a defect in mobilization could be suspected in these mice. We, therefore, set up a series of experiments where bone marrow $CD45^+$ cells (eg, depleted of stromal cells) from $Cav^{+/+}$ and $Cav^{-/-}$ mice were transplanted into lethally irradiated $Cav^{-/-}$ mice; $Cav^{+/+}$ mice were similarly transplanted to allow full comparison between the different combinations of donor and recipient mice. A 3-week delay was respected after transplantation to ensure the complete reconstitution of bone marrow; preliminary studies had shown that circulating leukocyte number and bone marrow integrity were back to normal 14 days after $CD45^+$ cell infusion. Figure 2A, left panels, shows that $Cav^{-/-}$ mice recovered from the ischemic insult when $CD45^+$ cells from wild-type mice, but not from $Cav^{-/-}$ mice, were used to reconstitute the bone marrow. In $Cav^{+/+}$ background animals (Figure 2A, right panels), the reconstitution of bone marrow also led to distinct patterns of response according to the origin of $CD45^+$ cells, although to a lesser extent than in $Cav^{-/-}$ animals. Accordingly, when $Cav^{-/-}$ $CD45^+$ cells were used, the restoration of blood flow in the proximal operated limb was delayed when compared with wild-type $CD45^+$-reconstituted mice (see Figure 2A, right panels). In fact, whereas in the latter mice, no distal limb atrophy was detectable, the loss of toes or the entire foot of the operated leg was consistently observed in $Cav^{-/-}$ $CD45^+$-reconstituted wild-type mice. These morphological alterations were less prominent, however, than in $Cav^{-/-}$ $CD45^+$-reconstituted $Cav^{-/-}$ mice; a complete leg atrophy occurred in a majority of these mice (5 of 6).

Based on the above results, besides the transplanted mouse background, the origin of bone marrow seemed also critical for postischemic revascularization (eg, no or delayed recovery with $CD45^+$ cells originated from $Cav^{-/-}$ mice). We therefore repeated the above experiments by using CM-DiI–labeled $CD45^+$ cells to reconstitute the bone marrow of irradiated mice (see Figure I in the online data supplement) and to further track the progenitor cell homing in the ischemic hindlimb. In $Cav^{-/-}$ mice (Figure 2B, left panels), progenitor cells derived from the $Cav^{-/-}$ $CD45^+$ cell transplantation were found heterogeneously distributed across the ischemic muscle and, in total, much less

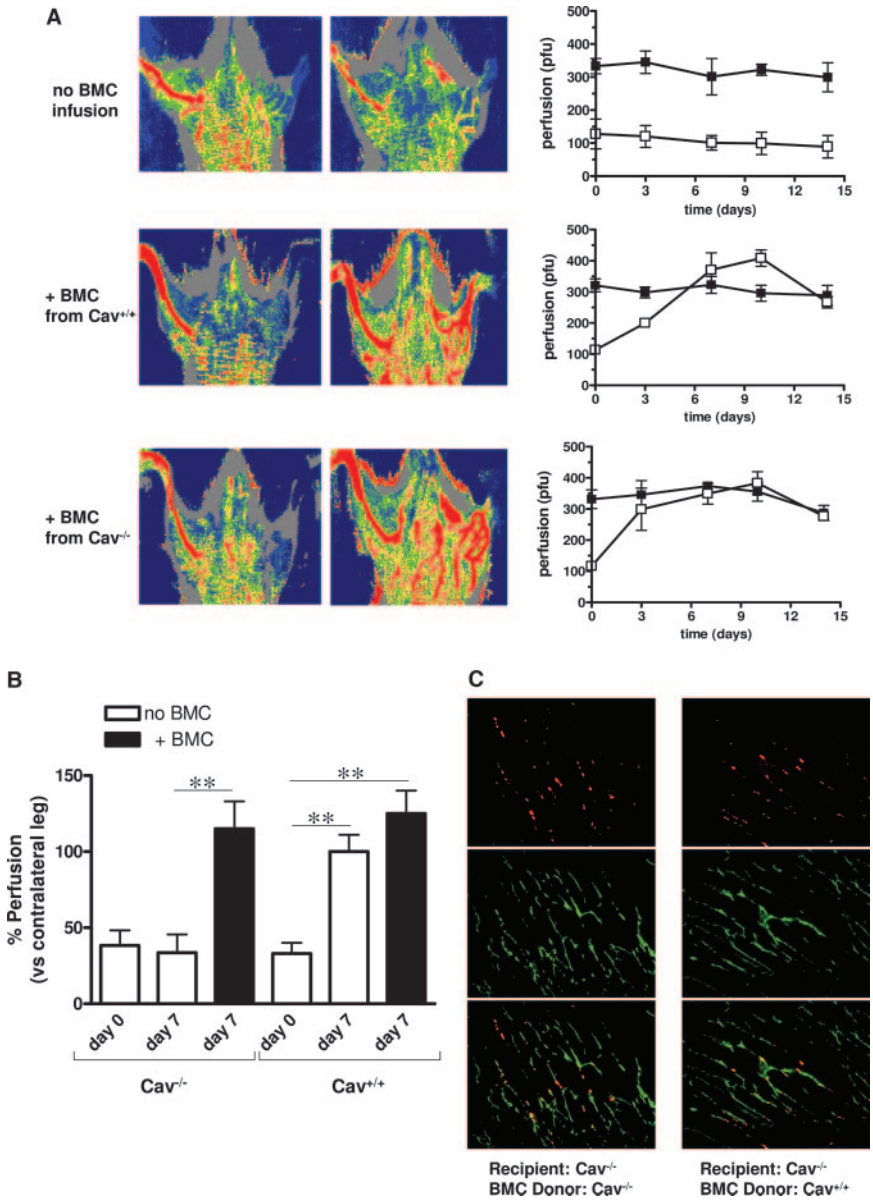

Figure 1. Sca-1$^+$ Lin$^-$ progenitor cell infusion rescues ischemic hindlimb in Cav$^{-/-}$ mice. Femoral artery/vein resection was performed on Cav$^{+/+}$ or Cav$^{-/-}$ mice, followed 24 hours later by the infusion (or not) of Sca-1$^+$ Lin$^-$ bone marrow cells (BMC) issued either from Cav$^{+/+}$ or Cav$^{-/-}$ animals and labeled with CM-DiI. A, Typical laser Doppler images of blood flow in posterior hindlimbs of Cav$^{-/-}$ mice just after the resection (day 0) and at day 7, as well as the quantification, at several time points, of the perfusion (mean±SE) in control (closed symbols) and operated (open symbols) legs (n=6); some SE are smaller than symbols. B, Bar graph represents the extent of perfusion (mean±SE) in the operated leg of either Cav$^{+/+}$ or Cav$^{-/-}$ mice (expressed as percentage of perfusion in the contralateral leg) at day 0 and day 7 with or without Cav$^{+/+}$ BMC infusion (**P<0.01, n=6). C, Representative images of CM-DiI labeling (red) (eg, Sca-1$^+$ Lin$^-$ BMC) and CD31 immunostaining (green) in the adductor muscle of the operated leg of Cav$^{-/-}$ mice at day 7; superimposition of both images is also provided.

abundant than those arising from Cav$^{+/+}$ cell transplantation (see Figure 2C for quantitative analysis). In Cav$^{+/+}$ mice, although similar extents of CM-DiI–labeled progenitor cells issued either from Cav$^{+/+}$ or Cav$^{-/-}$ mice could be found in some regions of the adductor muscle (see Figure 2B, right panels), the distribution was less homogeneous in the latter condition. Accordingly, quantitative analyses of the all tissue sections revealed a lesser staining when progenitor cells were issued from Cav$^{-/-}$ CD45$^+$ cell transplantation (see bars 3 and 4 in Figure 2C).

The microvascular density (see CD31 immunolabeling in Figure 2B, lower panels) was significantly higher in both mouse strains when the CD45$^+$ donor mouse was from a wild-type background (see Figure 2D for quantitative analysis); colocalization of CM-DiI and CD31 was however very poor suggesting paracrine influence of progenitor cells instead of direct participation to the structure of new capillaries. Moreover, slight but statistically significant differences distinguish the animals from Cav$^{+/+}$ and Cav$^{-/-}$ backgrounds: (1) the extent of CM-DiI–labeled Cav$^{+/+}$ progenitor cells found in the ischemic muscle was larger in Cav$^{-/-}$ recipient (compare bars 2 and 4 in Figure 2C); (2) the extent of CD31–labeled cells was larger in Cav$^{+/+}$ background animals (compare bars 1 and 3 in Figure 2D).

Cav$^{-/-}$ EPC Are Resistant to SDF-1–Induced Detachment From Bone Marrow Stromal Cells

To further dissect the mechanism accounting for the defect in mobilization of Cav$^{-/-}$ BMC, we examined whether the MMP-9 and SDF-1 pathways were differently regulated in wild-type and caveolin-deficient mice. Zymography analyses of crude bone marrow extracts did not reveal significant differences in gelatinase activity (not shown), suggesting the absence of alterations in MMP-2 and -9 activities in Cav$^{-/-}$ mice. Furthermore, because we were anticipating alterations in the EPC phenotype more than in the bone marrow stroma (where most of MMP activity originates), we focused our attention on SDF-1/CXCL12 and its receptor CXCR4 located

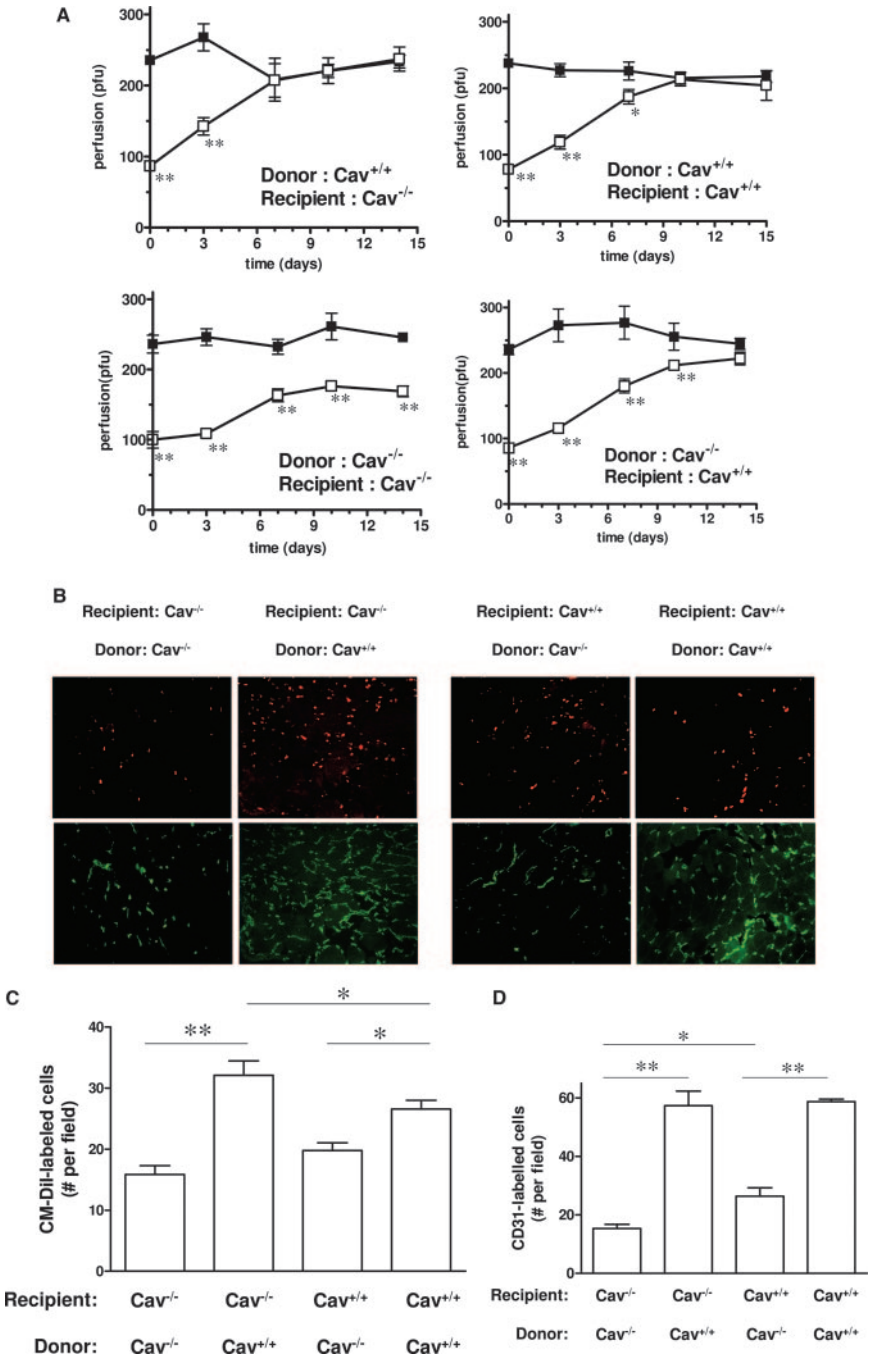

Figure 2. Caveolin gene deficiency is associated with a defect in mobilization of bone marrow cells. $Cav^{+/+}$ and $Cav^{-/-}$ (see recipients) were transplanted with $Cav^{+/+}$ or $Cav^{-/-}$ (see donors) $CD45^{+}$ BMC (labeled with CM-DiI) and submitted 3 weeks later to unilateral femoral artery/vein resection. A, Quantification of the perfusion (mean±SE) in control (closed symbols) and operated (open symbols) legs at several time points postresection; some SEs are smaller than symbols (*$P<0.05$, **$P<0.01$, vs corresponding value in contralateral leg; n=6). B, Representative pictures of CM-DiI labeling (red) (originally, $CD45^{+}$ BMC) and CD31 immunostaining (green) in the adductor muscle of the operated leg at day 7; heterogeneous distribution of labeled cells from $Cav^{-/-}$ donor across the muscle sections may account for discrepancies between corresponding pictures and numbers presented in subfigures C and D. Bar graphs represent the CM-DiI–labeled bone marrow-derived cells (C) and the CD31-immunostained vascular structures (D) in the 4 different combinations of donor/recipient. *$P<0.05$, **$P<0.01$ (n=6).

on EPC. Accordingly, we isolated stromal cells from $Cav^{-/-}$ and $Cav^{+/+}$ by negative selection ($CD45^{-}$) from total bone marrow and cultured them to confluence in the presence of serum. Stromal cell monolayers were then exposed to hypoxia (1% O_2 for 4 hours) to promote endogenous SDF-1 expression as previously documented.[23] Adhesion experiments were performed with EPC originating from both mouse genotypes, prechallenged or not with SDF-1. Figure 3A shows that when EPC were issued from $Cav^{+/+}$ mice, the SDF-1 treatment led to a decreased ability to adhere to stromal cells independently of their genotype (−85±7% and −72±10% with stromal cells from $Cav^{+/+}$ and $Cav^{-/-}$, respectively, versus untreated EPC; $P<0.01$, n=3). Conversely, $Cav^{-/-}$ EPC were resistant to SDF-1 stimulation and did not reveal significant reduction in adhesion when compared with untreated EPC (see also Figure 3B for quantitative analysis). In the same experimental set up, however, CXCR4 antibody blockade could abolish the $Cav^{+/+}$ and $Cav^{-/-}$ EPC adhesion on $Cav^{-/-}$ stromal cells to the same extent, further confirming the implication of the SDF-1/CXCR4 axis in the caveolin-mediated mobilization of EPC (Figure 3B). Fluorescence-activated cell sorting (FACS) analysis was then performed with EPC exposed or not to SDF-1 to examine the level of cell surface expression of the CXCR4 receptor, the SDF-1 cognate receptor. Although the total amounts of CXCR4 receptors were not significantly different in untreated

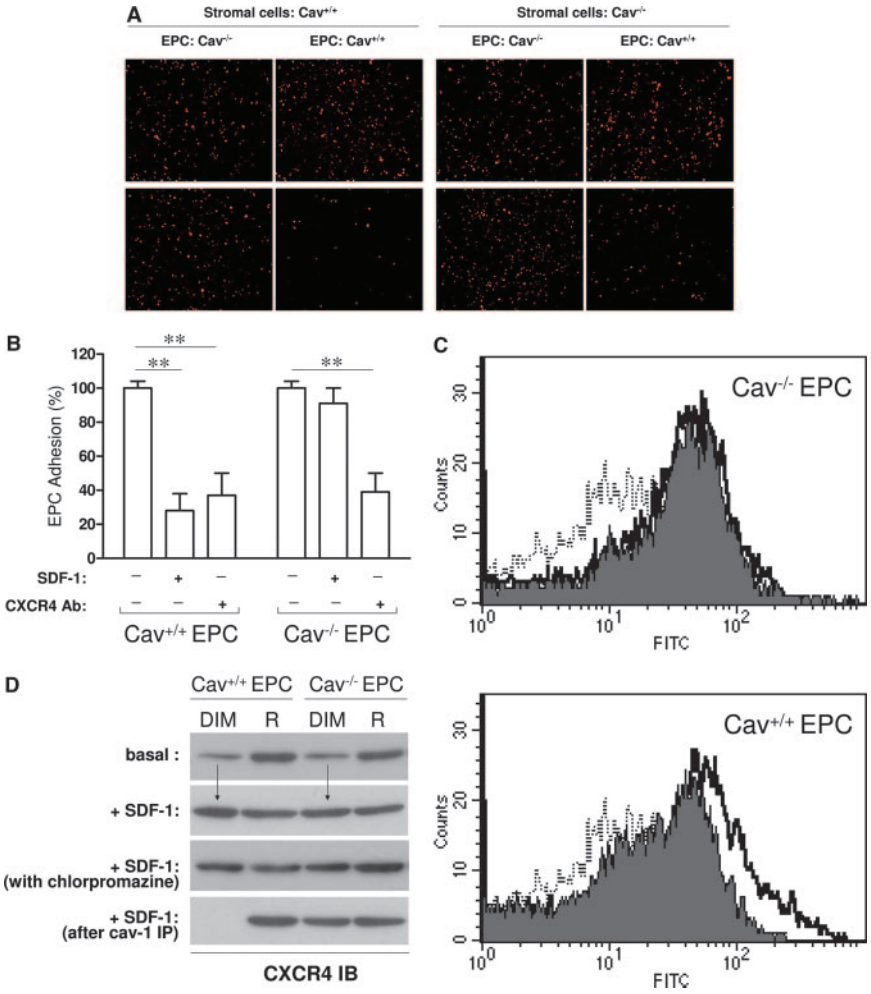

Figure 3. Caveolin expression is key for the SDF-1–induced egression of EPC from hypoxic stromal cells. A, Confluent monolayers of stromal cells preexposed to hypoxia (<1% O_2) for 4 hours were exposed to $Cav^{+/+}$ or $Cav^{-/-}$ EPC. Adhesion of $Cav^{+/+}$ or $Cav^{-/-}$ EPC (detected by red CM-DiI labeling) either untreated (top) or after exposure to 200 ng/mL SDF-1 for 20 minutes (bottom). B, Bar graph represents the extent (mean±SE) of adhesion (expressed as percentage of control) of $Cav^{+/+}$ and $Cav^{-/-}$ EPC in basal conditions, after SDF-1 exposure or incubation with a CXCR4 blocking antibody (**P<0.01, n=3). C, Representative FACS analysis of CXCR4 expression at the cell surface of $Cav^{-/-}$ (top) and $Cav^{+/+}$ (bottom) EPC; this experiment has been repeated twice with similar results. The bold black-delimited and shaded layouts correspond to the relative intensity of fluorescence (ie, abundance of CXCR4 receptors) before and after exposure to SDF-1 for 30 minutes, respectively; the dashed line represents the background cell fluorescence. D, CXCR4 immunoblottings (IB) were performed on detergent-insoluble membranes (DIM) and -soluble, remaining membranes (R) from $Cav^{+/+}$ and $Cav^{-/-}$ EPC. Basal and 30 minutes SDF-1–stimulated conditions are depicted; arrows point the increased CXCR4 signal in DIM after SDF-1 regardless of the EPC phenotype. These experiments were repeated twice with similar results. In 1 set of experiments, chlorpromazine (10 μg/mL) was used to block clathrin-coated pit formation and in another set, caveolin immunoprecipitation (IP) was first performed and only the IP supernatants were used for immunoblotting.

$Cav^{+/+}$ and $Cav^{-/-}$ EPC, the SDF-1 treatment did induce a shift to the left of the fluorescent peak in $Cav^{+/+}$ EPC, indicating the disappearance of part of CXCR4 receptors from the cell surface (Figure 3C). Such shift in fluorescence was not observed with SDF-1–treated $Cav^{-/-}$ EPC, thereby illustrating the resistance to internalization of CXCR4 when caveolin was absent (Figure 3C). We also performed CXCR4 immunoblotting on detergent-insoluble membranes enriched in rafts and caveolae, from both $Cav^{+/+}$ and $Cav^{-/-}$ EPC (Figure 3D). We found that in EPC from both origins, SDF-1 similarly induced the translocation of a large proportion of CXCR4 receptors to the detergent-insoluble fractions (approximately +40% of total CXCR4 receptors; see the shift between lanes 1 and 2 in Figure 3D). The implication of clathrin-coated pits was further excluded because the use of the cationic amphiphilic drug chlorpromazine, an inhibitor of clathrin-dependent, receptor-mediated endocytosis, failed to affect the CXCR4 internalization (Figure 3D). More importantly, when caveolin immunoprecipitation was performed to remove caveolar membranes (eg, to discriminate from rafts), the CXCR4 receptor could not be found in the remaining supernatant of $Cav^{+/+}$ EPC membranes, confirming the key role of caveolae in CXCR4 sequestration (see lane 4 in Figure 3D).

Ischemia Leads to an Increase in BMC Caveolin Expression and in Plasma SDF-1 Levels

Because the data presented above indicated a critical role of caveolin and SDF-1 in EPC mobilization, we examined how their expression evolved with time in situ. Accordingly, we used real time PCR to first compare the extent of caveolin-1 mRNA transcripts in Sca-1^+ Lin^- BMC collected at different time points after induction of hindlimb ischemia. Figure 4A shows that although caveolin-1 is almost absent from these hematopoietic cells in normal conditions, its expression rapidly increased in response to peripheral ischemia to reach a maximum after 7 days. The elevated level of caveolin expression in Sca-1^+ Lin^- BMC was maintained for 2 more weeks before rapidly dropping back to basal values. Finally, we examined whether cultured EPC also exhibited changes in caveolin abundance following in vitro exposure to serum and VEGF. Figure 4B shows that, indeed, the level of caveolin progressively increased to reach a maximum at day 14 of culture. Also, evaluation of circulating levels of SDF-1 revealed that in basal conditions, plasma levels of SDF-1 were 2-fold higher in $Cav^{-/-}$ than in $Cav^{+/+}$ mice. Following ischemic insult, the SDF-1 plasma levels increased in $Cav^{+/+}$ mice to reach the level of $Cav^{-/-}$ mice (Figure 4C). Interestingly, however, the amounts of circulating EPC (determined

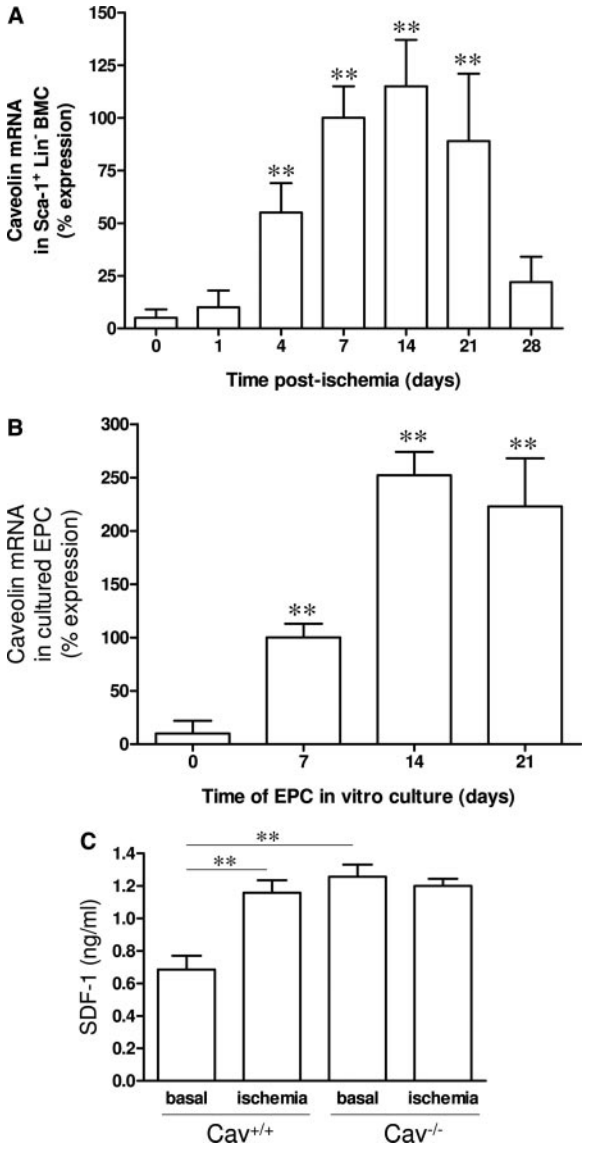

Figure 4. Ischemia-induced changes in caveolin in bone marrow-derived cells and in plasma SDF-1 abundance. A and B, The abundance of the caveolin-1 transcript was evaluated by real-time PCR from mRNA preparations issued from freshly isolated bone marrow Sca-1$^+$ Lin$^-$ cells (A) as well as from cultured EPC (B). The indicated time points correspond to the time where the cells were collected after induction of hindlimb ischemia and the time in culture after original isolation, respectively. Because the values at day 0 presented a large variability (mostly because of the limits of detection of this assay), the 100% value was arbitrarily fixed as the relative abundance of caveolin mRNA expression at day 7 (*$P<0.05$; **$P<0.01$, n=3). C, Levels of plasma SDF-1 in basal conditions as well as 24 hours after ischemia in Cav$^{+/+}$ and Cav$^{-/-}$ mice. **$P<0.01$ (n=4).

by numeration of colonies) appeared to be 41±19% higher in Cav$^{+/+}$ mouse plasma (versus Cav$^{+/+}$ mice; $P<0.01$, n=7).

Lack of Caveolin Increases the EPC Adhesion to Endothelial Cells

We next examined whether alterations in the caveolin-mediated CXCR4 internalization, which translated in a defect in mobilization from the bone marrow, also impacted the peripheral recruitment of progenitor cells by the endothelium of ischemic tissues. For this purpose, we used HUVEC that we coated with recombinant SDF-1 and then exposed to EPC to promote attachment through CXCR4. In basal conditions, the extent of EPC attachment was found to be consistently higher when issued from the Cav$^{-/-}$ background (+37±13% versus Cav$^{+/+}$ EPC; $P<0.05$, n=3) (see Figure 5A and 5B). This adhesion assay also revealed a significantly different pattern when EPC were first exposed to soluble SDF-1 before plating on SDF-1–coated endothelial cells. Indeed, the SDF-1 prechallenge led to a 80% decrease in Cav$^{+/+}$ EPC adhesion ($P<0.01$, n=3), whereas the attachment of Cav$^{-/-}$ EPC was not significantly altered (versus unstimulated Cav$^{-/-}$ EPC) (see Figure 5A and 5B). To further confirm the crucial role of caveolin in the adhesiveness of EPC, we transfected EPC from Cav$^{-/-}$ animals with a caveolin-encoding plasmid, and, conversely, EPC from Cav$^{+/+}$ animals were transduced with caveolin small interfering RNA (siRNA). Caveolin recombinant expression in Cav$^{-/-}$EPC reached the level of endogenous caveolin in Cav$^{+/+}$ EPC, whereas after siRNA treatment, caveolin amounted to ≈15% of the endogenous expression in Cav$^{+/+}$ EPC (see Figure 5C). Importantly, these acute modifications of Cav$^{+/+}$ and Cav$^{-/-}$ EPC phenotypes recapitulated the observations made with EPC issued from Cav$^{-/-}$ and Cav$^{+/+}$ mice, respectively. Accordingly, the reduction in caveolin expression led to a greater adhesion of SDF-1–treated wild-type EPC, and the reexpression of caveolin in Cav$^{-/-}$ EPC dramatically reduced their adhesion capacity in response to SDF-1 (Figure 5C).

Transient Decrease in Caveolin Expression Increases the Vasculogenic Potential of EPC

Finally, we reasoned that the infusion of EPC transiently deprived of caveolin/caveolae should improve their recruitment capacity in ischemic tissues and thereby lead to therapeutic advantages (versus nonmodified EPC). To examine this hypothesis, we treated 1-week cultured EPC with caveolin siRNA to decrease caveolin abundance as described above: the resulting caveolin downregulation (see Figure 5C) was maximal 24 hours after transfection and maintained for the next 36 hours (not shown). To avoid any confounding defects in angiogenesis in Cav$^{-/-}$ mice (versus postnatal vasculogenesis), we induced ischemic hindlimb by femoral artery/vein resection in wild-type animals and examined the ability of EPC treated or not with caveolin siRNA to rescue the limb perfusion. In these wild-type animals, the ischemia-induced neovascularization was very efficient in the adductor muscle around the ligated vessels and hampered the search for biological differences induced by either transduced or nonmodified EPC. We therefore focused on the perfusion and tissue integrity distal from the thigh ligature (eg, in the foot) in the weeks following femoral vessel resection. We found that by infusing caveolin siRNA-transduced EPC, blood flow in the foot from the operated limb was restored to a larger extent than with native EPC infusion (Figure 6A). Similarly, the alterations in both the tissue integrity and an index of the active use of the foot, evaluated by arbitrary scoring, were more extensively corrected with caveolin siRNA-transduced EPC than with sham-transfected EPC (see Figure 6B and 6C).

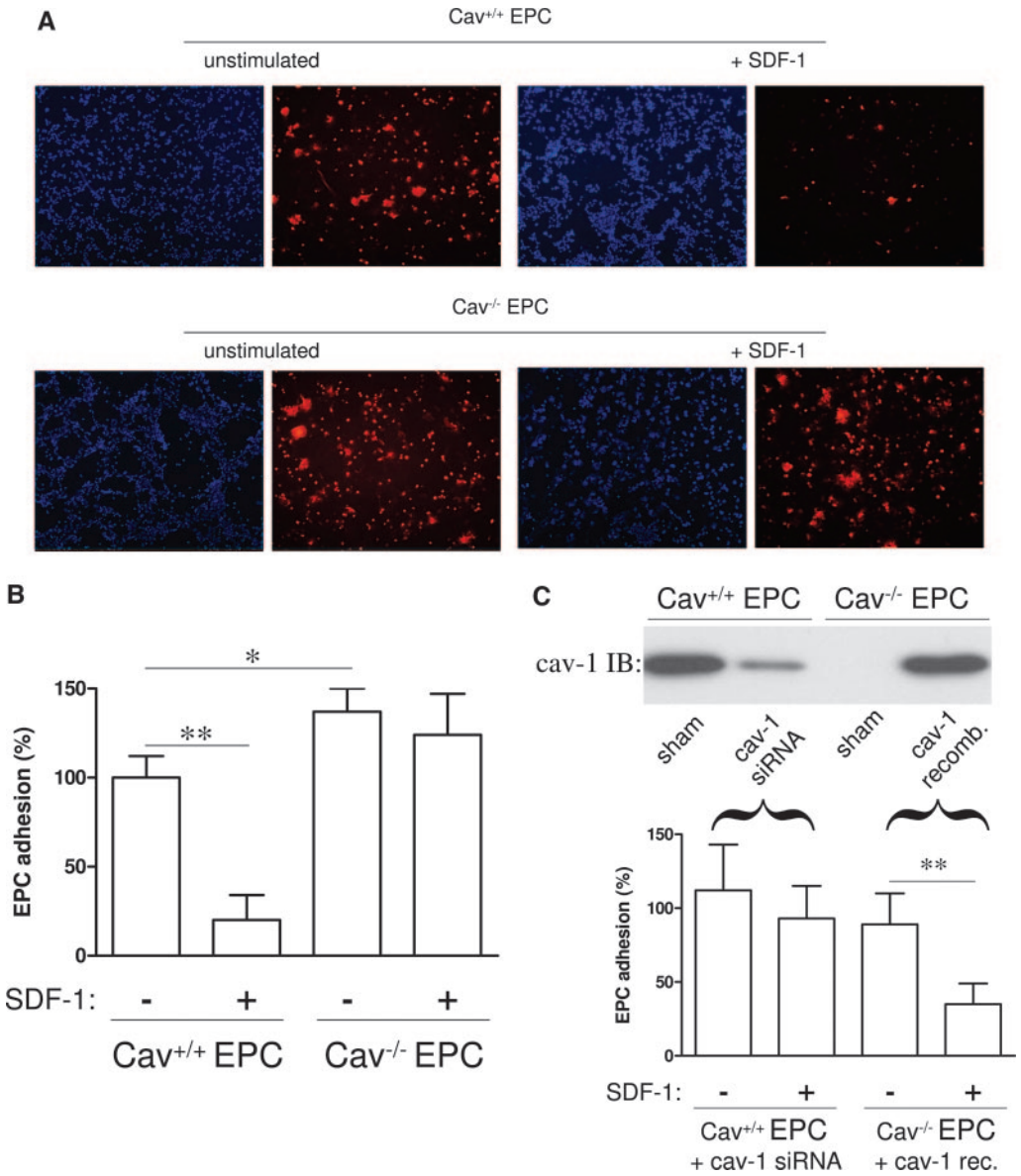

Figure 5. Caveolin gene deficiency is associated with an increase in attachment to SDF-1–presenting endothelial cells. Confluent monolayers of endothelial cells precoated with SDF-1 were exposed to $Cav^{+/+}$ or $Cav^{-/-}$ EPC pretreated or not with 200 ng/mL SDF-1 for 20 minutes. A, DAPI staining (blue) of EC monolayers (authenticating similar confluence level between the different conditions) and the extent of $Cav^{+/+}$ (top) or $Cav^{-/-}$ (bottom) EPC adhesion (detected by red CM-DiI labeling). B and C, Bar graphs represent the extent of adhesion (expressed as percentage of control) of $Cav^{+/+}$ and $Cav^{-/-}$ EPC in basal condition or after SDF-1 exposure (B) and the extent of adhesion (expressed as percentage of controls) of $Cav^{-/-}$ and $Cav^{+/+}$ EPC expressing recombinant caveolin or transduced by caveolin siRNA, respectively (C). Corresponding changes in caveolin expression were validated by Western blotting (see above bar graph).*$P<0.05$, **$P<0.01$ (n=3).

Discussion

Although many reports using transgenic animals have revealed that the nature of the bone marrow stroma may dramatically influence the progenitor cell mobilization step, the current study emphasizes that the EPC phenotype itself may directly influence their ability to be mobilized. Accordingly, we showed that a defect in caveolin expression could prevent SDF-1–induced internalization of the CXCR4 receptors and the consecutive release of EPC from the bone marrow to the blood circulation. The previously reported defect in postischemic angiogenesis in caveolin-deficient mice,[7] therefore, appears to be aggravated by a defect in postnatal vasculogenesis, further highlighting the potential impact of changes in caveolin abundance observed in cardiovascular diseases.[20] Furthermore, we found that by reproducing this phenomenon (eg, caveolin downregulation) on isolated, cultured EPC through a caveolin siRNA-based strategy, the SDF-1–dependent homing of progenitor cells to endothelial cells was stimulated and the contribution of postnatal vasculogenesis increased in a model of ischemic tissue reperfusion. These apparently paradoxical data underscore 2 sides of the same coin: caveolae are needed for SDF-1–induced CXCR4 internalization and, although blocking this process in the bone marrow hampers the mobilization of progenitor cells, the transient inhibition of CXCR4 sequestration in isolated, cultured EPC increases their homing capacity in ischemic tissues.

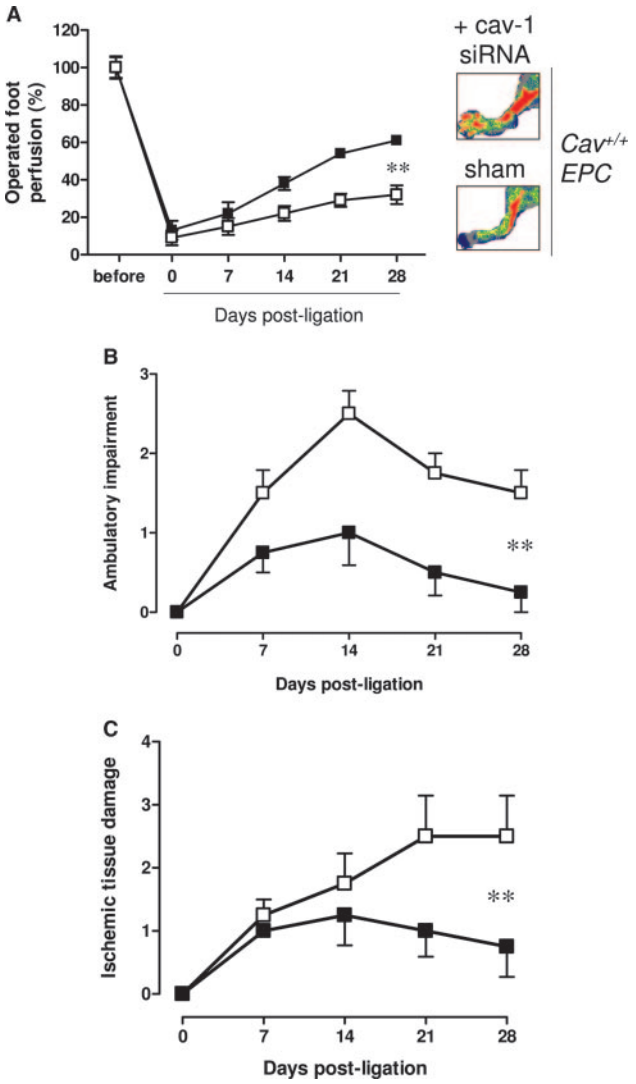

Figure 6. Caveolin knocking down improves the EPC capacity of restoring blood flow and tissue integrity and function after hindlimb ischemia. Femoral artery/vein resection was performed in $Cav^{+/+}$ mice, followed 24 hours later by the infusion of EPC. A, Laser Doppler imaging (LDI) quantification of blood flow in the foot of the operated hindlimb (expressed as a % of the blood flow in the nonischemic foot), before and after the ligature (day 0) and at several time points following EPC infusion. EPC were either transduced with caveolin siRNA (closed symbols) or sham transfected (open symbols) (n=5); some SEs are smaller than symbols. Representative color-coded LDI pictures at day 28 are shown for both conditions. Functional and morphological assessments of ischemic limb are also presented over follow-up, as the scoring of the ambulatory impairment (B) and ischemic tissue damages (C). $^{**}P<0.01$, at day 28 (n=5).

The cell surface expression of the CXCR4 chemokine receptor is a major determinant in the homing capacity of hematopoietic stem and progenitor cells. There are several processes proposed to regulate the SDF-1–mediated mobilization of CXCR4-expressing cells from the bone marrow, including peptidase processing,[24,25] ubiquitination and lysosomal sorting,[26] and desensitization[23,27] of the CXCR4 receptor. In the current study, we identified the SDF-1–stimulated internalization of CXCR4 receptors within caveolae as a critical mode of mobilization from the bone marrow. Indeed, FACS analysis revealed a net decrease in the extent of surface CXCR4 receptors in $Cav^{+/+}$ but not $Cav^{-/-}$ EPC following soluble SDF-1 exposure. We further provided evidence that the disruption of the CXCR4 direct interaction with SDF-1–expressing stromal cells was involved and not the signaling pathways potentially regulated by caveolin. Previous reports[28,29] have shown that signaling downstream SDF-1 is associated with CXCR4 receptor redistribution to rafts (at the leading edge of migrating cells), eventually followed by their internalization. In our study, when isolating detergent-insoluble membranes (essentially made of rafts and caveolae) from the rest of the cell extracts, we found a similar shift of SDF-1–induced CXCR4 receptors toward these detergent-insoluble fractions from both $Cav^{+/+}$ and $Cav^{-/-}$ EPC (Figure 3D). In $Cav^{+/+}$ EPC, the detergent-insoluble CXCR4 was further associated to caveolin (as determined by immunoprecipitation), indicating that internalization but not clustering of CXCR4 was altered in $Cav^{-/-}$ EPC. We further documented that in experiments aiming to evaluate the chemotactic potential of SDF-1, no difference could be found between the migratory potential of $Cav^{+/+}$ and $Cav^{-/-}$ EPC (see supplemental Figure II). Altogether, our data indicate that the caveolin deficiency does not impact the SDF-1–mediated signaling but alters the endocytosis-based dissociation of CXCR4-expressing EPC from SDF-1–decorated stromal cells.

Other groups have identified the formation of clathrin-coated pits as the pathway of CXCR4 receptor internalization.[26,30,31] In these studies, however, the authors were using either non–primary transfected cells[31] or cells known not to express caveolin/caveolae such as lymphoid cells.[30,31] In a more recent study, however, Dar et al reported that SDF-1 could be internalized through clathrin-coated pits and resecreted by bone marrow endothelial and stromal cells.[32] Although the clathrin-dependent CXCR4 transcytosis was convincingly documented in this study, the authors did not provide evidence to exclude other routes (such as the caveolae fission), and, more importantly, they reported that for leukocytes and hematopoietic stem cells (that are more parented to the EPC used in our study), clathrin-coated pits were not involved for the transcytosis of SDF-1. Finally, it is worth mentioning that in another situation involving bone marrow mobilization, namely exposure to the cytotoxic 5-FU chemotherapeutic drug, a significant delay in bone marrow reconstitution was observed in $Cav^{-/-}$ mice (not shown), thereby extending the critical role of caveolin/caveolae in the process of BMC trafficking. In this context, the elevated basal levels of plasma SDF-1 in $Cav^{-/-}$ mice (see Figure 4C) may also be interpreted as a compensatory response to a general deficit in HSC mobilization.

Finally, our study reveals that the engagement of progenitor cells in the endothelial lineage is strikingly initiated in the bone marrow. Caveolin expression, as needed for the caveolae sequestration of activated CXCR4 sequestration, is, indeed, induced in the bone marrow on induction of peripheral ischemia. Quantitative evaluation of caveolin mRNA expression in wild-type animals revealed that the abundance of caveolin in hematopoietic cells progressively increased after femoral artery/vein resection. Interestingly, culture of EPC in "endothelial cell growth medium" also revealed a progressive increase in caveolin abundance, suggesting a shift in the phenotype of these cells and their propensity to engage in a "more differentiated" endothelial lineage. Of potential therapeutic interest is the

observation that transduction of wild-type EPC with caveolin siRNA to transiently alter caveolae formation allows to exploit a time frame during which progenitor cells are particularly prone to adhere to SDF-1–presenting compartments but after which caveolin-dependent signaling pathways may still occur.

In summary, the present work demonstrates for the first time a critical role of the structural protein caveolin for the EPC mobilization from the bone marrow and the consecutive revascularization of ischemic tissues. The SDF-1 binding to CXCR-4 is, indeed, finely regulated by the caveolar sequestration process, allowing the detachment of progenitor cells from bone marrow stromal cells in the presence of an excess soluble SDF-1 (originating from ischemic tissues). Besides the elucidation of this mechanism that finely regulates the egression of matured progenitor cells, our data also pave the way for the therapeutic exploitation of caveolin targeting (ie, downregulation through siRNA use) to increase the engraftment potential of progenitor and hematopoietic stem cells.

Acknowledgments

This work was supported by grants from the Belgian National Fund for Scientific Research (FNRS), the Belgian Federation against Cancer, the J. Maisin Foundation, an Action de Recherche Concertée (ARC 04/09-317) from the Communauté Française de Belgique, and a Pôle d'Attraction Interuniversitaire (PAI). O.F. and C.D. are FNRS Research Associates.

References

1. Isner JM, Asahara T. Angiogenesis and vasculogenesis as therapeutic strategies for postnatal neovascularization. *J Clin Invest*. 1999;103:1231–1236.
2. Losordo DW, Dimmeler S. Therapeutic angiogenesis and vasculogenesis for ischemic disease. Part I: angiogenic cytokines. *Circulation*. 2004;109:2487–2491.
3. Asahara T, Kawamoto A. Endothelial progenitor cells for postnatal vasculogenesis. *Am J Physiol Cell Physiol*. 2004;287:C572–C579.
4. Carmeliet P. Angiogenesis in health and disease. *Nat Med*. 2003;9:653–660.
5. Rafii S, Lyden D. Therapeutic stem and progenitor cell transplantation for organ vascularization and regeneration. *Nat Med*. 2003;9:702–712.
6. Urbich C, Dimmeler S. Endothelial progenitor cells: characterization and role in vascular biology. *Circ Res*. 2004;95:343–353.
7. Sonveaux P, Martinive P, DeWever J, Batova Z, Daneau G, Pelat M, Ghisdal P, Gregoire V, Dessy C, Balligand JL, Feron O. Caveolin-1 expression is critical for vascular endothelial growth factor-induced ischemic hindlimb collateralization and nitric oxide-mediated angiogenesis. *Circ Res*. 2004;95:154–161.
8. Brouet A, DeWever J, Martinive P, Havaux X, Bouzin C, Sonveaux P, Feron O. Antitumor effects of in vivo caveolin gene delivery are associated with the inhibition of the proangiogenic and vasodilatory effects of nitric oxide. *FASEB J*. 2005;19:602–604.
9. Bauer PM, Yu J, Chen Y, Hickey R, Bernatchez PN, Looft-Wilson R, Huang Y, Giordano F, Stan RV, Sessa WC. Endothelial-specific expression of caveolin-1 impairs microvascular permeability and angiogenesis. *Proc Natl Acad Sci U S A*. 2005;102:204–209.
10. Gratton JP, Lin MI, Yu J, Weiss ED, Jiang ZL, Fairchild TA, Iwakiri Y, Groszmann R, Claffey KP, Cheng YC, Sessa WC. Selective inhibition of tumor microvascular permeability by cavtratin blocks tumor progression in mice. *Cancer Cell*. 2003;4:31–39.
11. Gu Z, Kaul M, Yan B, Kridel SJ, Cui J, Strongin A, Smith JW, Liddington RC, Lipton SA. S-nitrosylation of matrix metalloproteinases: signaling pathway to neuronal cell death. *Science*. 2002;297:1186–1190.
12. Feron O, Kelly RA. The caveolar paradox: suppressing, inducing, and terminating eNOS signaling. *Circ Res*. 2001;88:129–131.
13. Wei Y, Yang X, Liu Q, Wilkins JA, Chapman HA. A role for caveolin and the urokinase receptor in integrin-mediated adhesion and signaling. *J Cell Biol*. 1999;144:1285–1294.
14. Frank PG, Lee H, Park DS, Tandon NN, Scherer PE, Lisanti MP. Genetic ablation of caveolin-1 confers protection against atherosclerosis. *Arterioscler Thromb Vasc Biol*. 2004;24:98–105.
15. Upla P, Marjomaki V, Kankaanpaa P, Ivaska J, Hyypia T, Van Der Goot FG, Heino J. Clustering induces a lateral redistribution of alpha 2 beta 1 integrin from membrane rafts to caveolae and subsequent protein kinase C-dependent internalization. *Mol Biol Cell*. 2004;15:625–636.
16. Ge S, Pachter JS. Caveolin-1 knockdown by small interfering RNA suppresses responses to the chemokine monocyte chemoattractant protein-1 by human astrocytes. *J Biol Chem*. 2004;279:6688–6695.
17. Razani B, Woodman SE, Lisanti MP. Caveolae: from cell biology to animal physiology. *Pharmacol Rev*. 2002;54:431–467.
18. Parton RG, Richards AA. Lipid rafts and caveolae as portals for endocytosis: new insights and common mechanisms. *Traffic*. 2003;4:724–738.
19. Feron O, Dessy C, Moniotte S, Desager JP, Balligand JL. Hypercholesterolemia decreases nitric oxide production by promoting the interaction of caveolin and endothelial nitric oxide synthase. *J Clin Invest*. 1999;103:897–905.
20. Sbaa E, Frerart F, Feron O. The double regulation of endothelial nitric oxide synthase by caveolae and caveolin: a paradox solved through the study of angiogenesis. *Trends Cardiovasc Med*. 2005;15:157–162.
21. Drab M, Verkade P, Elger M, Kasper M, Lohn M, Lauterbach B, Menne J, Lindschau C, Mende F, Luft FC, Schedl A, Haller H, Kurzchalia TV. Loss of caveolae, vascular dysfunction, and pulmonary defects in caveolin-1 gene-disrupted mice. *Science*. 2001;293:2449–2452.
22. Vasa M, Fichtlscherer S, Adler K, Aicher A, Martin H, Zeiher AM, Dimmeler S. Increase in circulating endothelial progenitor cells by statin therapy in patients with stable coronary artery disease. *Circulation*. 2001;103:2885–2890.
23. Ceradini DJ, Kulkarni AR, Callaghan MJ, Tepper OM, Bastidas N, Kleinman ME, Capla JM, Galiano RD, Levine JP, Gurtner GC. Progenitor cell trafficking is regulated by hypoxic gradients through HIF-1 induction of SDF-1. *Nat Med*. 2004;10:858–864.
24. Sadir R, Imberty A, Baleux F, Lortat-Jacob H. Heparan sulfate/heparin oligosaccharides protect stromal cell-derived factor-1 (SDF-1)/CXCL12 against proteolysis induced by CD26/dipeptidyl peptidase IV. *J Biol Chem*. 2004;279:43854–43860.
25. Valenzuela-Fernandez A, Planchenault T, Baleux F, Staropoli I, Le Barillec K, Leduc D, Delaunay T, Lazarini F, Virelizier JL, Chignard M, Pidard D, Arenzana-Seisdedos F. Leukocyte elastase negatively regulates stromal cell-derived factor-1 (SDF-1)/CXCR4 binding and functions by amino-terminal processing of SDF-1 and CXCR4. *J Biol Chem*. 2002;277:15677–15689.
26. Marchese A, Benovic JL. Agonist-promoted ubiquitination of the G protein-coupled receptor CXCR4 mediates lysosomal sorting. *J Biol Chem*. 2001;276:45509–45512.
27. Shen H, Cheng T, Olszak I, Garcia-Zepeda E, Lu Z, Herrmann S, Fallon R, Luster AD, Scadden DT. CXCR-4 desensitization is associated with tissue localization of hemopoietic progenitor cells. *J Immunol*. 2001;166:5027–5033.
28. van Buul JD, Voermans C, van Gelderen J, Anthony EC, van der Schoot CE, Hordijk PL. Leukocyte-endothelium interaction promotes SDF-1-dependent polarization of CXCR4. *J Biol Chem*. 2003;278:30302–30310.
29. Nguyen DH, Taub D. CXCR4 function requires membrane cholesterol: implications for HIV infection. *J Immunol*. 2002;168:4121–4126.
30. Signoret N, Oldridge J, Pelchen-Matthews A, Klasse PJ, Tran T, Brass LF, Rosenkilde MM, Schwartz TW, Holmes W, Dallas W, Luther MA, Wells TN, Hoxie JA, Marsh M. Phorbol esters and SDF-1 induce rapid endocytosis and down modulation of the chemokine receptor CXCR4. *J Cell Biol*. 1997;139:651–664.
31. Venkatesan S, Rose JJ, Lodge R, Murphy PM, Foley JF. Distinct mechanisms of agonist-induced endocytosis for human chemokine receptors CCR5 and CXCR4. *Mol Biol Cell*. 2003;14:3305–3324.
32. Dar A, Goichberg P, Shinder V, Kalinkovich A, Kollet O, Netzer N, Margalit R, Zsak M, Nagler A, Hardan I, Resnick I, Rot A, Lapidot T. Chemokine receptor CXCR4-dependent internalization and resecretion of functional chemokine SDF-1 by bone marrow endothelial and stromal cells. *Nat Immunol*. 2006;6:1038–1046.

Expanded Materials and Methods:

Animal experiments. Caveolin-deficient ($Cav^{-/-}$) mice[1] (originally obtained from Dr T.V. Kurzchalia, Max Planck Institute for Molecular Cell Biology and Genetics, Dresden, Germany) and their control littermate ($Cav^{+/+}$) were generated through heterozygous matings and housed in our local facility. A minimum of 6 backcrossing has been perfomed before using the animals described in this study. We used 8-10 week-old animals that do not present macroscopic anomalies such as hyperproliferative lung parenchyma or hypertrophic heart. Each procedure was approved by the local authorities according to national animal care regulations. In all the experiments requiring validation of quantitative data discriminating the $Cav^{+/+}$ and $Cav^{-/-}$ genotypes, two blinded investigators have interpreted the results.

Ischemic Hindlimb Reperfusion Assay. Anesthetized mice were anesthetized and after local fur removal using a depilatory cream, were placed on a heating pad (37°C) to minimize temperature variations. Blood flow in the ligated and control opposite legs was measured with a Laser Doppler perfusion imager (LDI, Moor Instruments), as previously described.[2] Perfusion was evaluated on the basis of colored histogram pixels and normalized for the limb surface analysed.

Assessment of ischemic limb function and local tissue damage. Semiquantitative assessment of impaired use of the ischemic limb was performed according to the following scoring scale: 3=dragging of foot, 2=no dragging but no plantar flexion, 1=plantar flexion, and 0=flexing the toes to resist gentle traction on the tail. Semiquantitative measurement of the ischemic damage was also assessed by scoring:

4=any amputation, 3=severe discoloration or subcutaneous tissue loss or necrosis, 2=moderate discoloration, 1=mild discoloration, and 0=no difference from the contralateral hindlimb. Two blinded observers assigned all scores.

Bone marrow and endothelial progenitor cells. Bone marrow (BM) was harvested aseptically by flushing mouse femurs and tibias with phosphate-buffered saline containing 5% fetal calf serum. For endothelial progenitor cell (EPC) production, BM mononuclear cells were directly cultured on fibronectin-coated flasks, as previously described,[3] using endothelial cell growth medium (EGM, Clonetics) supplemented with 100 ng/mL vascular endothelial growth factor (VEGF) (R&D systems) and 25% FCS. The identity of EPC was confirmed by morphological analysis (typical clusters and cord-like structures), DiI-acLDL (Molecular Probes), FITC-labeled *Ulex europaeus* lectin and von Willebrand factor (vWF) stainings (Sigma). EPC were used at day 7 after initial seeding except when indicated otherwise. In a series of experiments, EPC were transfected, as previously described,[2] with caveolin-1-encoding plasmid or caveolin siRNA. For bone marrow transplantation, recipient mice were lethally irradiated (8.5 Gy) and received an intravenous injection of 2 x 10^6 $CD45^+$ BMC 24 hours after irradiation.

Immunohistochemistry and cell tracking. CD31 antibody staining was performed to label the vasculature in the adductor muscle of the ischemic leg, as previously described.[2] In some experiments, injected cells including $CD45^+$ cells used for bone marrow transplantation and Sca-1^+ Lin^- cells (see above), were labeled with the long-lasting cell tracker CM-DiI (Molecular Probes) according to the manufacturer's instructions. However, in the transplantation experiments, because of the progressive dilution of CM-DiI during the bone marrow reconstitution, we limited our

investigation to the tracking of BMC in the first 4 weeks post-transplantation. For quantitative analyses, CM-DiI-labeled cells were counted in randomly chosen fields of tissue sections or cell culture wells; 5 different fields were considered per condition.

EPC adhesion on endothelial and stromal cells. HUVEC (Clonetics) were cultured in EGM till confluence in 96-well plates, coated for 20 min with SDF-1 (100 ng/mL) and then exposed to EPC for 2 hours at 37°C. At the end of the experiment, non-adherent EPC were removed by aspiration and HUVEC were then washed three times with PBS. Similar experiments were performed on stromal cells isolated by negative selection ($CD45^-$) from total bone marrow and cultured in DMEM (containing 10% FCS for at least 2 weeks). Before exposure to EPC, stromal cells were subjected to hypoxia (1% O_2) in order to promote endogenous SDF-1 expression, as previously documented.[4] To determine the amounts of adherent cells, EPC were pre-labeled with CM-DiI, as detailed above. In some experiments, EPC were pre-mixed with neutralizing anti-CXCR4 antibody and in others, pre-incubated for 20 min with SDF-1 (100-500 ng/mL). CXCR4 internalization was examined by FACS analysis using a FITC-conjugated anti-CXCR4 antibody (Pharmingen). In another series of experiments, EPC were first transfected, as previously described,[2] with caveolin-1-encoding plasmid or caveolin siRNA (sequence: aagatgtgattgcagaaccag); β-galactosidase-encoding plasmid and unrelated siRNA were used as controls, respectively.

EPC migration. Modified Boyden chambers with 8-µm pore-size filters were used to evaluate EPC migration. EPC were seeded at a density of $5x10^4$ per well and were allowed to migrate for 5 hours at 37°C. Recombinant SDF-1 was diluted in EBM-2

medium and placed in the lower chamber of the modified Boyden chamber. After migration, cells on the bottom of the filter were stained with Giemsa solution and counted manually in random fields.

Real-time PCR. Total RNA was extracted using Trizol reagent (Life Technologies) and cDNA was synthesized using random hexamers and Superscript First-strand reverse transcriptase (Invitrogen). Real-time quantitative PCR analyses were performed in triplicate using SYBR Green PCR Master Mix (Applied Biosystems) and the following specific primers: caveolin-1 sense, 5'-tttaccgcttgttgtctacga-3'; caveolin-1 antisense, 5'-tatctctttctgcgtgctga-3'; HPRT sense, 5'- tgctgacctgctggattaca-3'; HPRT antisense, 5'-ttttatgtcccccgttgact-3'. PCR fluorescence data were obtained and analysed with the ABI PRISM 5700 System instrument (PE Applied Biosystems). Ct (number of cycles needed to generate a fluorescent signal above a predefined threshold) were determined for each sample and the relative caveolin mRNA expression, expressed as fold-variation over control, was calculated using the $2^{-\Delta\Delta Ct}$ formula after normalization to HPRT (ΔCt) and determination of the difference in Ct ($\Delta\Delta$Ct) between the various conditions tested.

Detergent-insoluble membrane isolation. EPC were lysed in ice-cold TNE buffer (25 mmol/L Tris, 150 mmol/L NaCl, and 1 mmol/L EGTA) containing a cocktail of protease inhibitors (Sigma). After 10 passages through 23G and 26G needles, postnuclear supernatants were obtained after centrifugation at 800*g* at 4°C for 10 minutes. PNS was then incubated with 1% Triton at 4°C for 30 minutes under constant agitation and the detergent-soluble and insoluble fractions separated by centrifugation.

Immunoblotting. EPC membrane extracts (crude homogenates, detergent-insoluble and –soluble membranes) were immunoblotted with caveolin-1 or CXCR4 antibodies. In some experiments, caveolin immunoprecipitation (IP) was perfomed first and immunoblotting carried out on the IP supernatant left behind; both caveolin and CXCR4 antibodies were from BD PharMingen.

ELISA test. SDF-1 determination was performed by SDF-1 enzyme-linked immunosorbent assay (ELISA) kit (R&D systems) according to the manufacturer's instruction using 100 µl undiluted mouse plasma.

Statistical analysis. Data are normalized to control condition and are presented for convenience as mean ± SE. Statistical analyses were made using Student *t* test or 2-way ANOVA where appropriate.

References.

1. Drab M, Verkade P, Elger M, Kasper M, Lohn M, Lauterbach B, Menne J, Lindschau C, Mende F, Luft FC, Schedl A, Haller H, Kurzchalia TV. Loss of caveolae, vascular dysfunction, and pulmonary defects in caveolin-1 gene-disrupted mice. *Science*. 2001;293:2449-2452.

2. Sonveaux P, Martinive P, DeWever J, Batova Z, Daneau G, Pelat M, Ghisdal P, Gregoire V, Dessy C, Balligand JL, Feron O. Caveolin-1 expression is critical for vascular endothelial growth factor-induced ischemic hindlimb collateralization and nitric oxide-mediated angiogenesis. *Circ Res*. 2004;95:154-161.

3. Vasa M, Fichtlscherer S, Adler K, Aicher A, Martin H, Zeiher AM, Dimmeler S. Increase in circulating endothelial progenitor cells by statin therapy in patients with stable coronary artery disease. *Circulation*. 2001;103:2885-2890.

4. Ceradini DJ, Kulkarni AR, Callaghan MJ, Tepper OM, Bastidas N, Kleinman ME, Capla JM, Galiano RD, Levine JP, Gurtner GC. Progenitor cell trafficking is regulated by hypoxic gradients through HIF-1 induction of SDF-1. *Nat Med*. 2004;10:858-864.

Online Supplement Figure 1.

CMDiI-labelled bone marrow 4 weeks after transplantation. For BM transplantation, recipient mice were lethally irradiated (8.5 Gy) and received an intravenous injection of 2 x 10^6 $CD45^+$ BMC 24 hours after irradiation. Infused cells were pre-labeled with the long-lasting cell tracker CM-DiI (Molecular Probes) according to the manufacturer's instructions. Background fluorescence (non-transplanted bone marrow) is presented in the right panel for information.

Online Supplement Figure 2.

The lack of caveolin does not alter SDF-1-induced EPC chemotaxis. $Cav^{+/+}$ and $Cav^{-/-}$ EPC were seeded on the upper level of a modified Boyden chamber and allowed to migrate for 5 hours in the presence (or not) of 200 ng/mL SDF-1 in the bottom compartment. Bar graph represents the numbers (mean ± SE) of migrated cells per high powered field (**P<0.01, n=8).

Online Supplementary Figure 1.

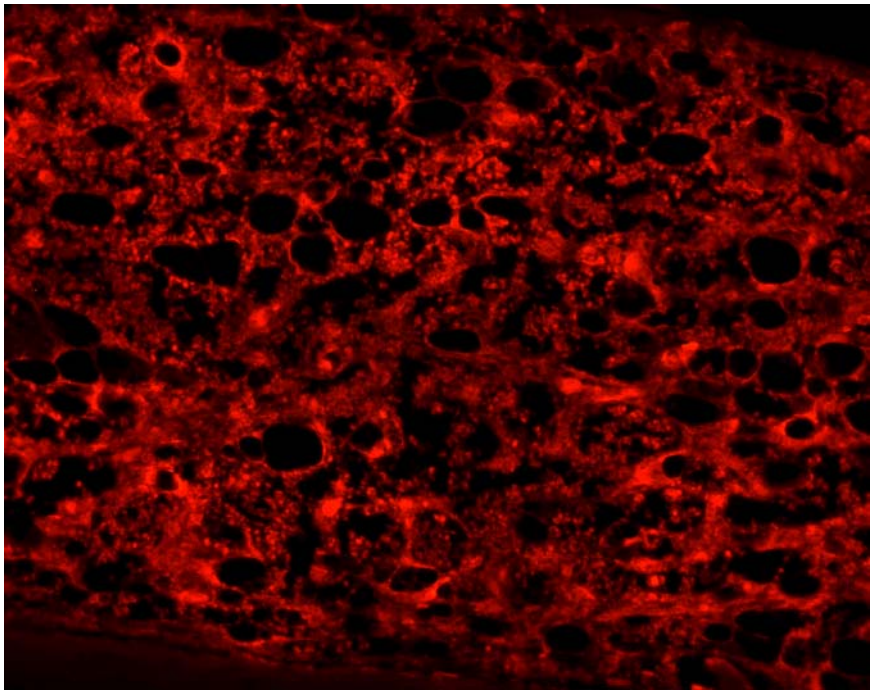

CM-Dil (day 28 post-transpl.)

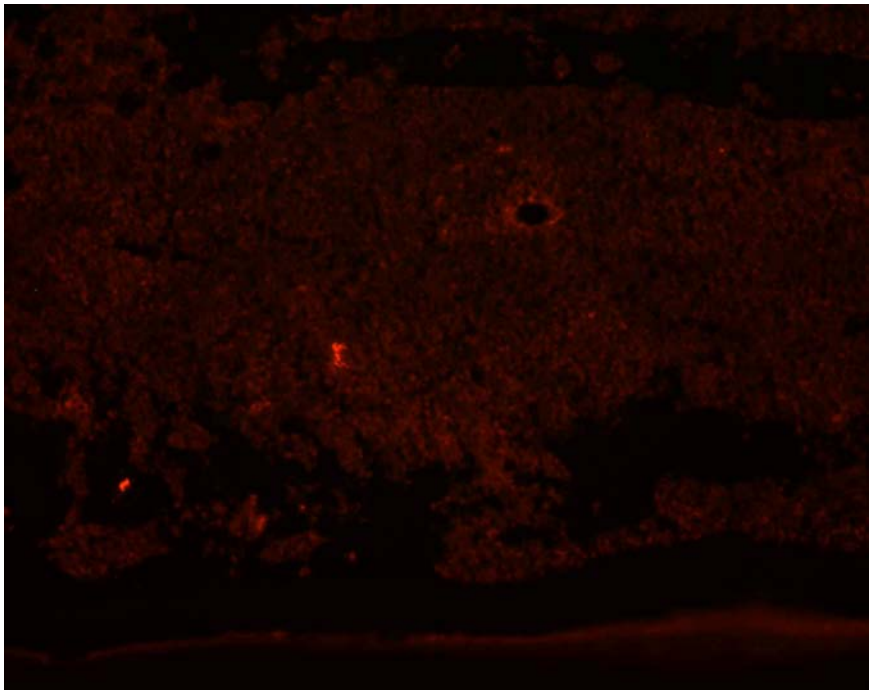

Background Fluorescence

Online Supplementary Figure 2.